

# CHAPTER IV

## RESULTS AND DISCUSSION

### 4.1 Characterization of Supported Tungsten Catalysts

#### 4.1.1 XRD Results

Phase analysis of SBA-15 support synthesized was carried out by XRD technique. The XRD pattern for as-synthesized SBA-15 is shown in Figure 4.1 where three well-resolved peaks were observed. Assignment of those peaks are known as (100), (110) and (200) reflections, respectively. Peaks positions are located in a quite low  $2\theta$  values due to lack of short-range order of the structure. After calcination in air at 500°C for 10 h, the XRD pattern shows that the hexagonal morphology is preserved with increasing peak intensity resulted from removing of organic template from the mesopores and all of peaks appear at slightly larger  $2\theta$  values. Three peaks are still observed confirming that the hexagonal structure of SBA-15 is thermally stable, although the unit cell contracted after removal of organic template by calcination.

When tungsten was loaded into SBA-15 support by incipient wetness impregnation method. All samples show lower intensity of (100) reflection and vanished peaks of (110) and (200) reflections as shown in Figure 4.2. This might be due to disturbance of order of host structure by interaction between tungsten species and support. As found that XRD peak intensity is very sensitive to several parameters such as moisture, template existence, temperature and duration of calcinations. This is accounted by the presence of long-range order of its structure but the absence of short-range order as

found in normal crystalline materials. SEM is selected to be a tool for following up the information of SBA-15 instead of XRD.

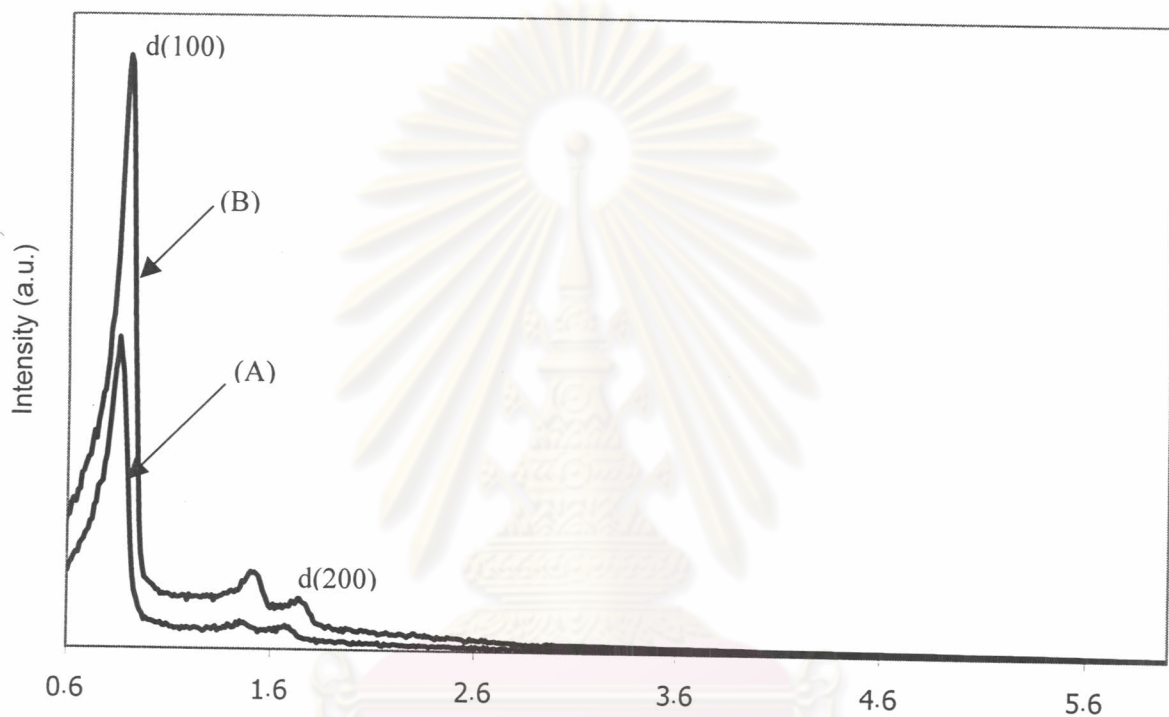


**Figure 2.1** XRD patterns of (A) as-synthesized SBA-15 and (B) calcined SBA-15

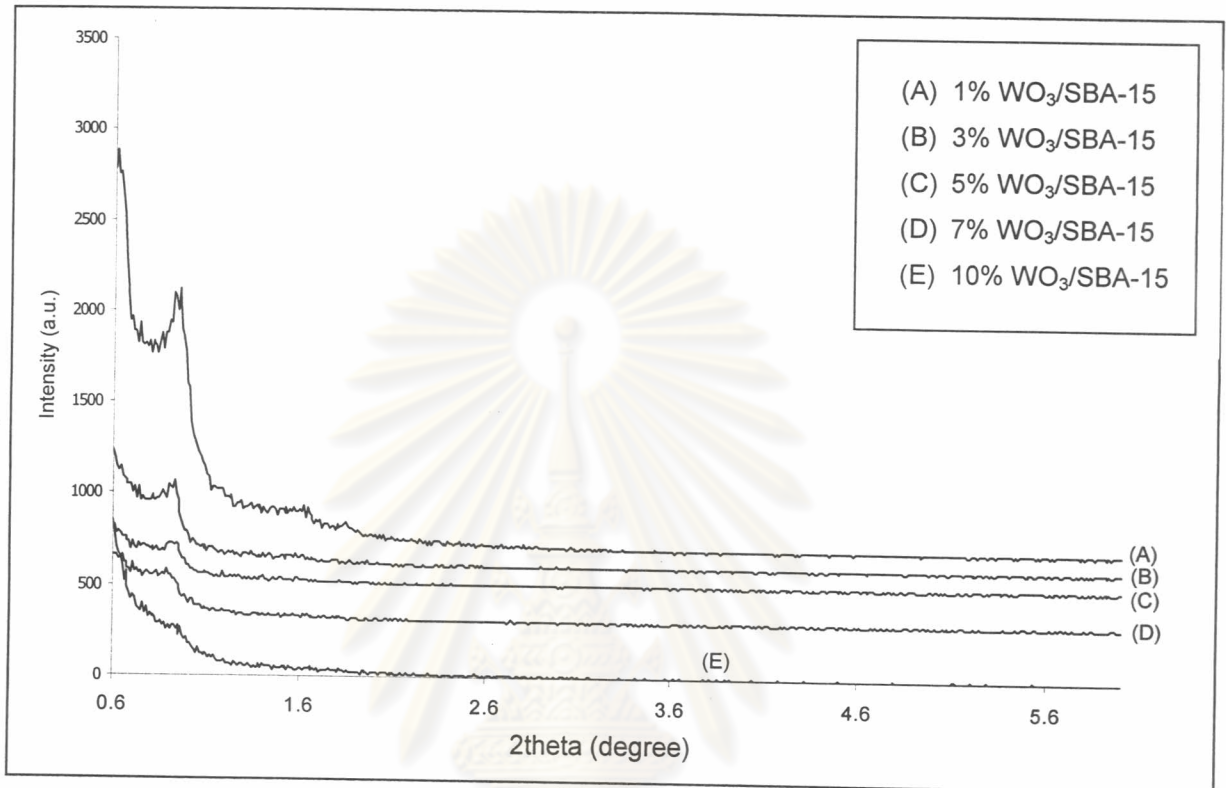


**Figure 4.2** XRD patterns of WO<sub>3</sub>/SBA-15 at various WO<sub>3</sub> loadings

ศูนย์วิทยทรัพยากร  
จุฬาลงกรณ์มหาวิทยาลัย

### 4.1.2 Scanning Electron Microscopy

Scanning electron microscopic (SEM) images reveal that the as-synthesized SBA-15 consists of many rope-like domains (Figure 4.3 (B) and (C)), which are aggregated into wheat-like macrostructures as shown in Figure 4.3 (A).

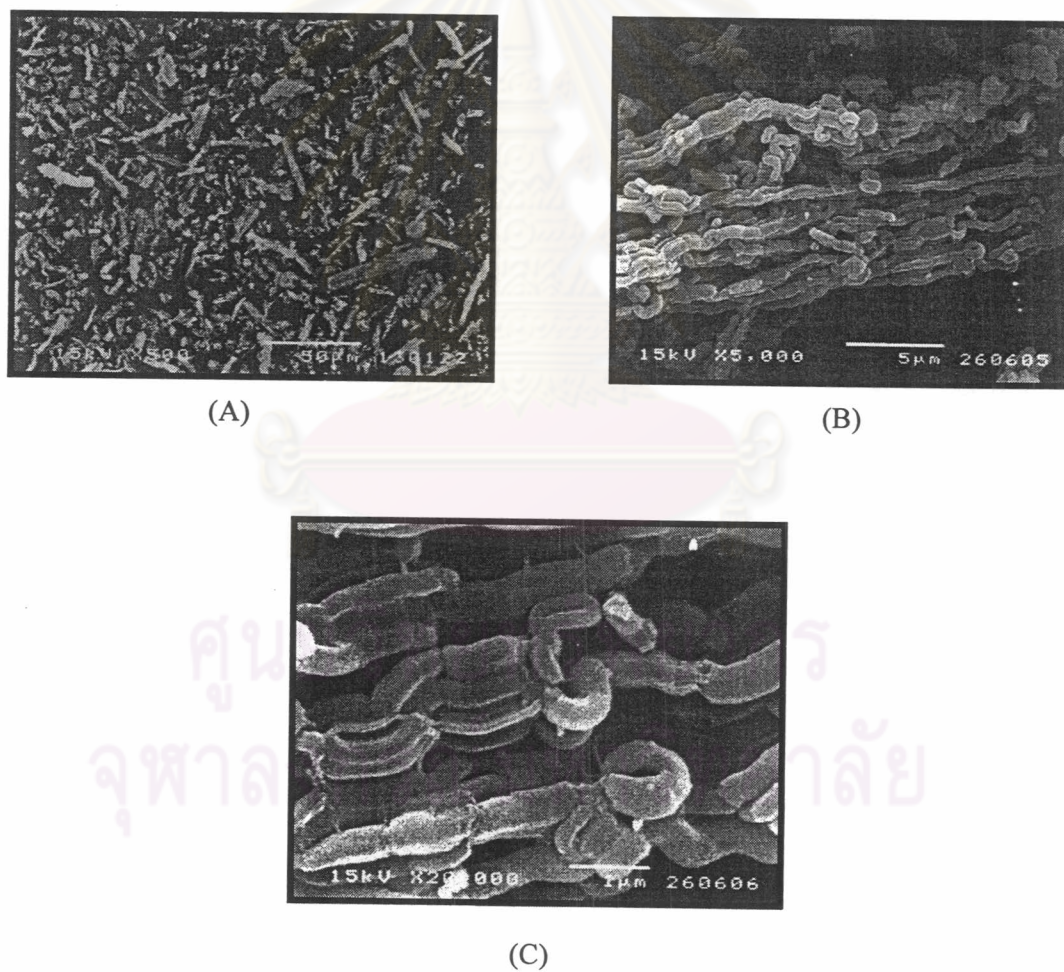


**Figure 4.3** SEM images of pure silica SBA-15 with (A) x 500, (B) x 5,000 and (C) x 20,000 magnification

Tungsten species distributions on SBA-15 support are illustrated by SEM-EDX as shown in Figure 4.4. These images show the remained rope-like morphologies but decrease of wheat-like particle size due to disturbing from loaded tungsten and it indicates that tungsten species are highly dispersed on the SBA-15 support. High disperse of tungsten species on the support corresponding to white dot in picture could be obtained by impregnation method.

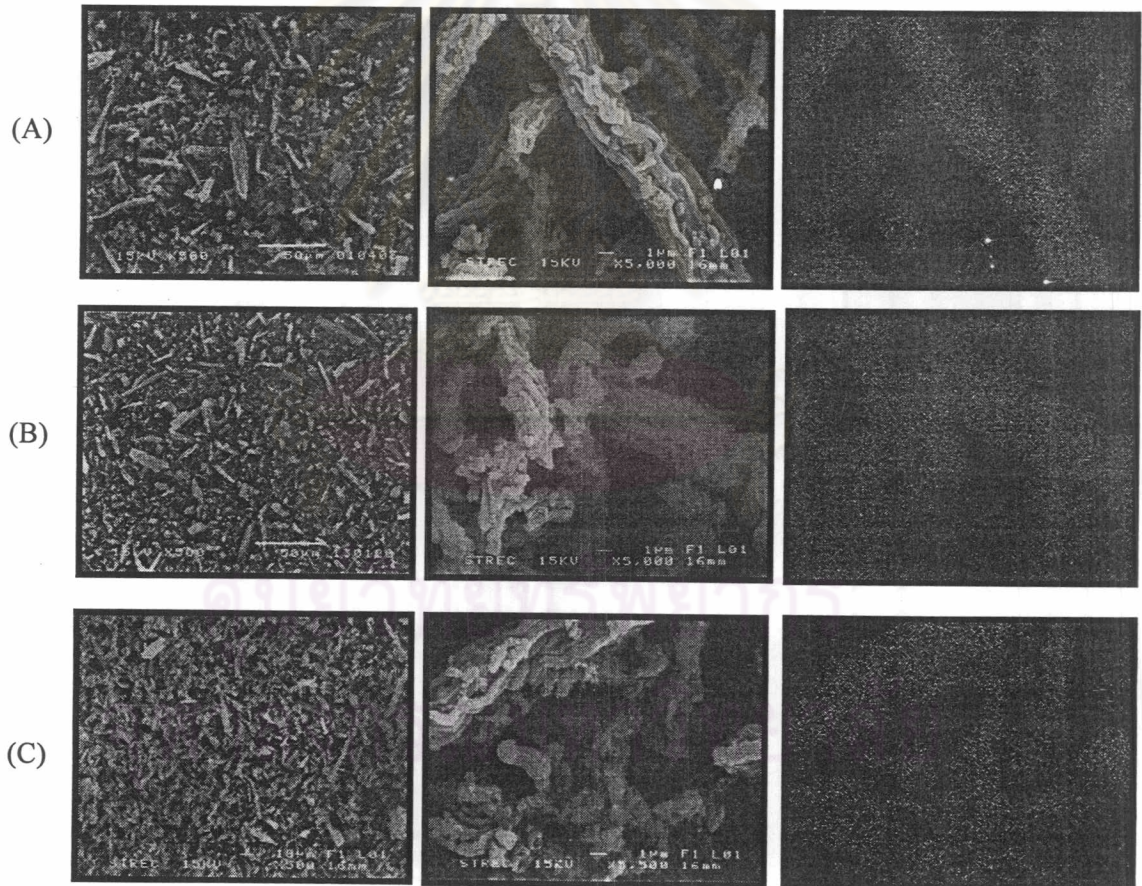


**Figure 4.4** SEM image vs. X-ray mapping of (A) 1%  $\text{WO}_3/\text{SBA-15}$ , (B) 5%  $\text{WO}_3/\text{SBA-15}$  and (C) 10%  $\text{WO}_3/\text{SBA-15}$

### 4.1.3 BET Specific Surface Area

Nitrogen adsorption-desorption isotherms of the SBA-15 and WO<sub>3</sub>/SBA-15 was shown in Figure 4.5. Samples of SBA-15, 1% and 3% WO<sub>3</sub>/SBA-15 exhibit a well-expressed hysteresis loop of type IV which is the characteristic pattern of mesoporous materials while high loadings of 5%, 7% and 10% WO<sub>3</sub>/SBA-15 do not show typical mesoporosity adsorption behavior. BET specific surface area of SBA-15 support and WO<sub>3</sub>/SBA-15 catalyst are listed in Table 4.1. Tungsten loading results in a decrease of surface area of SBA-15 support with increasing tungsten loading. This is attributed to the loss in crystallinity seen in the XRD patterns due to the tungsten oxide species.

**Table 4.2** BET specific surface area of SBA-15 and WO<sub>3</sub>/SBA-15 catalysts

Sample	BET Specific surface area (cm <sup>2</sup> /g)
SBA-15	779
1% WO <sub>3</sub> /SBA-15	535
3% WO <sub>3</sub> /SBA-15	412
5% WO <sub>3</sub> /SBA-15	329
7% WO <sub>3</sub> /SBA-15	243
10% WO <sub>3</sub> /SBA-15	104

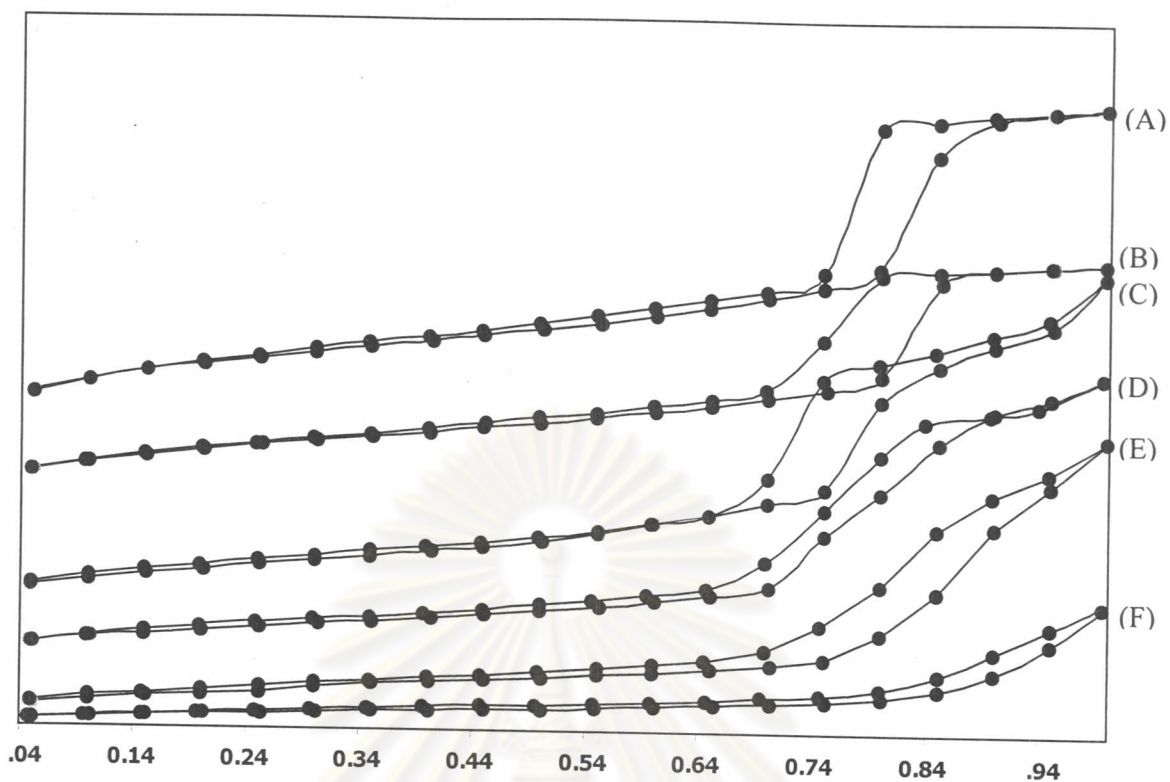


**Figure 4.5**  $N_2$  adsorption-desorption isotherm of (A) SBA-15, (B) 1%  $WO_3$ /SBA-15, (C) 3%  $WO_3$ /SBA-15, (D) 5%  $WO_3$ /SBA-15, (E) 7%  $WO_3$ /SBA-15, and (F) 10%  $WO_3$ /SBA-15

Considering pore size distribution of bare SBA-15 support and  $WO_3$ /SBA-15 in Figure 4.6, narrow pore size distribution was found for SBA-15 support at maximum value of 96 Å. When tungsten was loaded on SBA-15 in small amount, 1% and 3%  $WO_3$ /SBA-15, a slight decrease in pore size of SBA-15 support was observed. This might be due to impregnated metal oxide which are highly dispersed on surface of pores. However, high tungsten loadings of 5%, 7% and 10%  $WO_3$ /SBA-15 resulted in pore size increasing and broad pore size distribution. It indicates that some of the pore structure of SBA-15 support was collapsed by high loaded tungsten. Moreover, the remain pore structure was covered by large amount of tungsten oxide, resulting in pore size decreasing as present over range of 10-100 Å in Figure 4.6 (F).

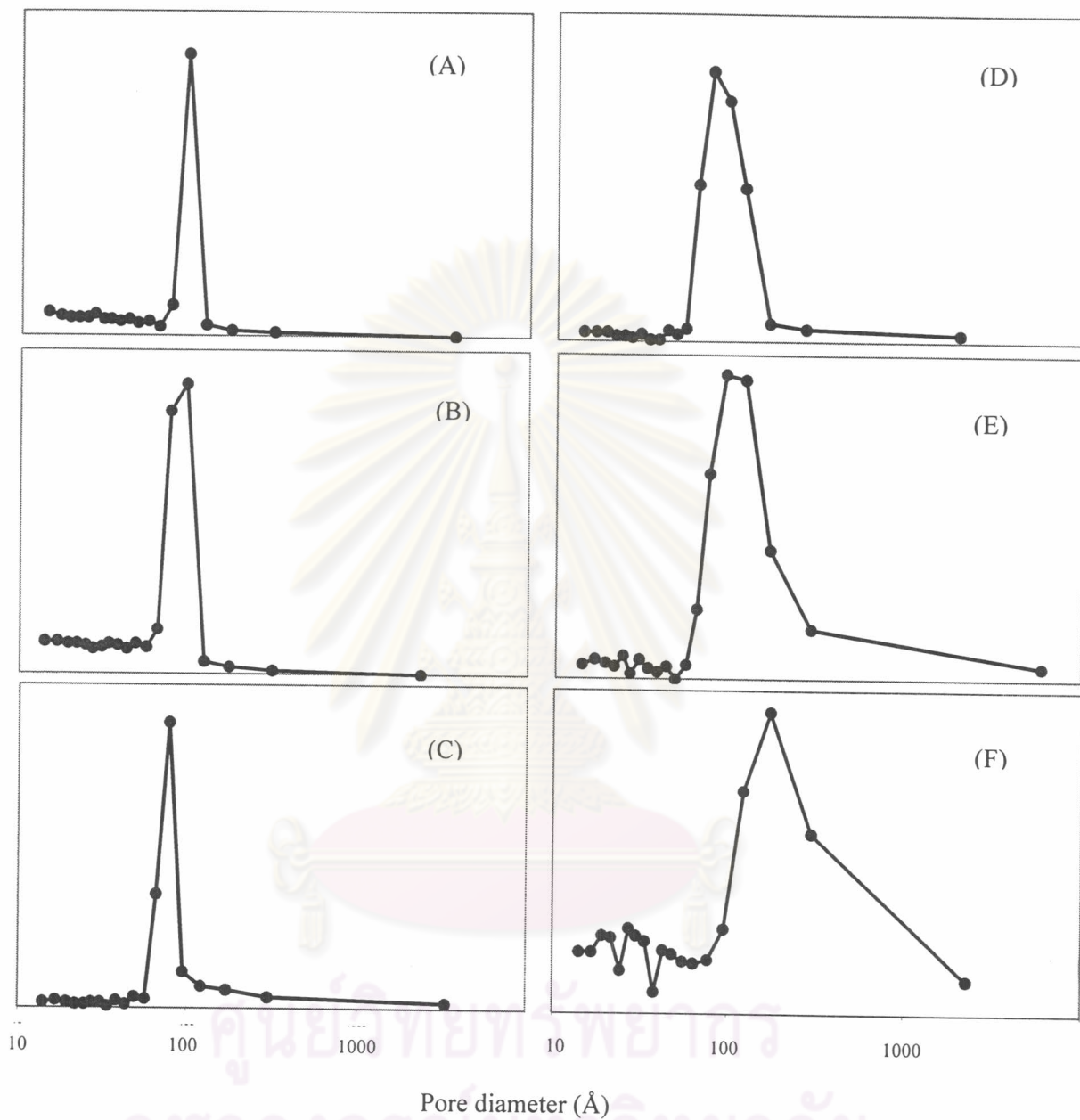


**Figure 4.6** Pore size distribution of (A) SBA-15, (B) 1%  $\text{WO}_3/\text{SBA-15}$ , (C) 3%  $\text{WO}_3/\text{SBA-15}$ , (D) 5%  $\text{WO}_3/\text{SBA-15}$ , (E) 7%  $\text{WO}_3/\text{SBA-15}$ , and (F) 10%  $\text{WO}_3/\text{SBA-15}$



#### 4.1.4 DR-UV spectra

In the reference DR-UV spectra as shown in Figure 4.7, sodium tungstate represents tetrahedrally monomeric tungstate species, ammonium tungstate represents octahedrally polymeric tungstate species, and  $\text{WO}_3$  represents the bulk tungsten oxide. DR-UV spectra of various supported tungsten catalysts at 0, 1, 3, 5, 7 and 10%  $\text{WO}_3$  loading on SBA-15 are shown in Figure 4.8. The  $\text{WO}_3/\text{SBA-15}$  spectra are comparable with the reference spectrum of  $\text{Na}_2\text{WO}_4 \cdot 2\text{H}_2\text{O}$ . It can be concluded that all  $\text{WO}_3/\text{SBA-15}$  samples have the characteristics of tetrahedrally monomeric tungstate species on the supports.



ศูนย์วิจัยทรัพยากร  
จุฬาลงกรณ์มหาวิทยาลัย

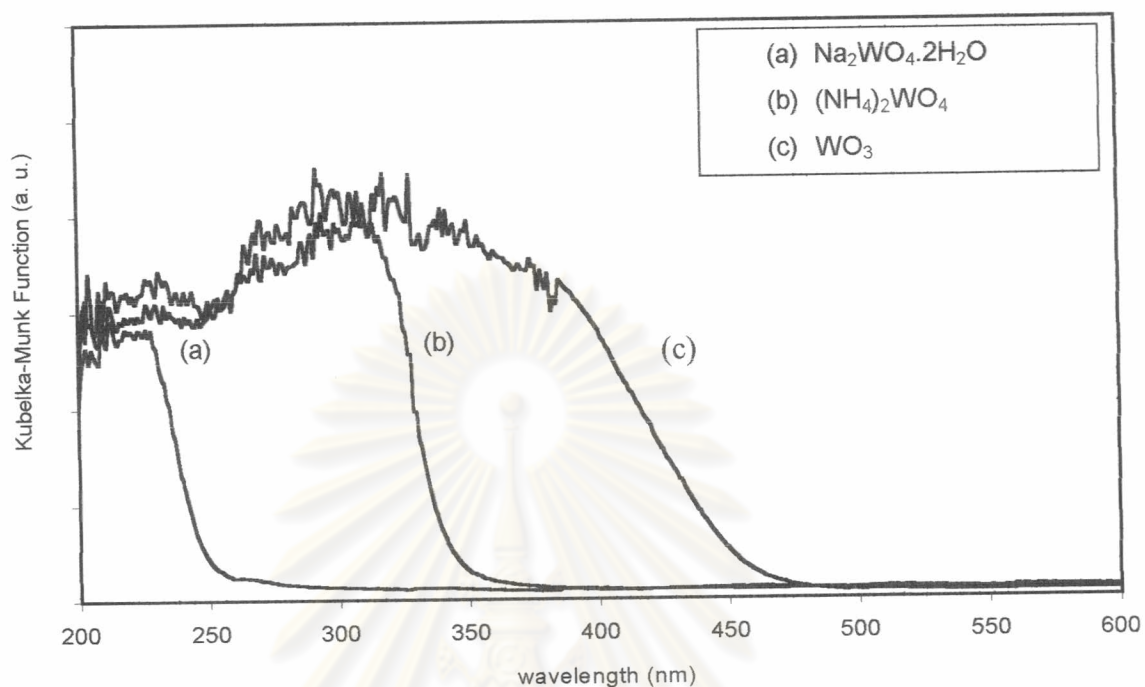


Figure 4.7 DR-UV spectra of reference tungstate species

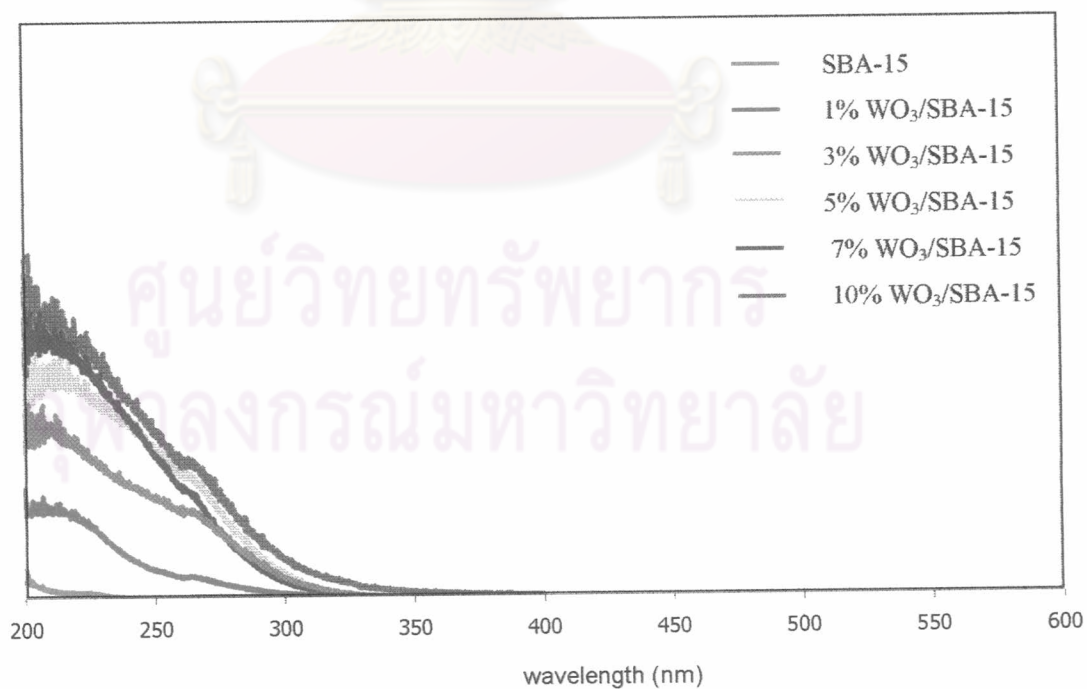
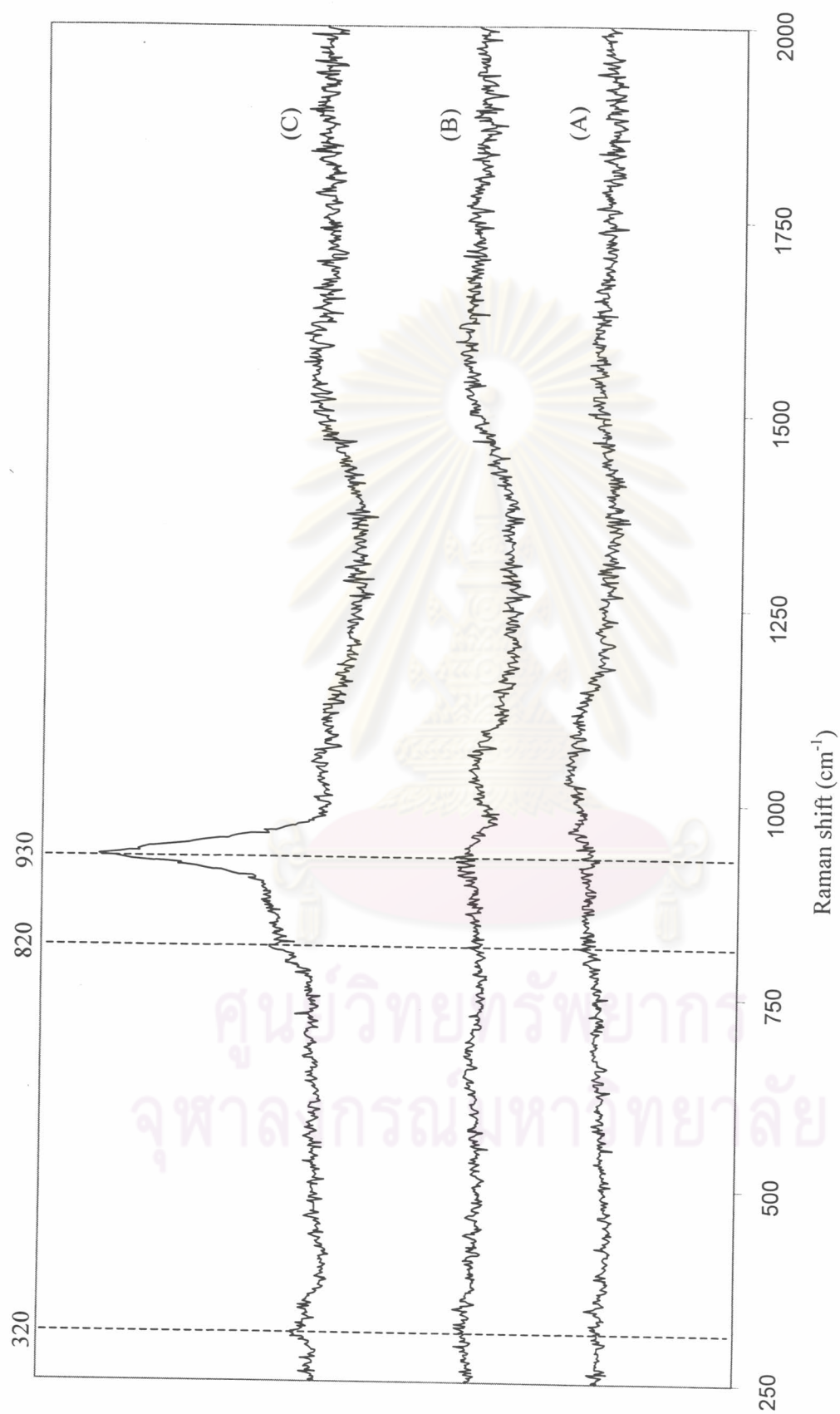


Figure 4.8 DR-UV spectra of SBA-15 and  $\text{WO}_3/\text{SBA-15}$  catalyst at various loadings of  $\text{WO}_3$

#### 4.1.5 Subtraction Laser Raman Spectra

The subtraction Raman spectra of  $\text{WO}_3/\text{SBA-15}$  catalysts by Raman spectrum of SBA-15 support are presented in Figure 4.9. As described in Figure 4.9, no significant band present in the Raman spectrum of 1%  $\text{WO}_3/\text{SBA-15}$  while the Raman spectra of 5%  $\text{WO}_3/\text{SBA-15}$  exhibits similar pattern with 1%  $\text{WO}_3/\text{SBA-15}$ . This indicates that high dispersion of tungsten oxide on SBA-15 support was presented over the range of 1-5%  $\text{WO}_3$ , leading to undetectability by Laser Raman scattering technique. At high tungsten loading, 10%  $\text{WO}_3/\text{SBA-15}$ , the Raman spectrum shows number of band differ from previous samples. It consists of band at 930 and 820  $\text{cm}^{-1}$  and a weak band at 320  $\text{cm}^{-1}$  which could describe that the band at 930 and 820  $\text{cm}^{-1}$  refer to stretching mode of W-O bond of tetrahedrally coordinated tungsten oxide species on support and the weak band at 320  $\text{cm}^{-1}$  refers to bending mode of W-O bond of hydrate tungstic oxide ( $\text{WO}_3 \cdot \text{H}_2\text{O}$ ). This result is agreement in DR-UV results.

ศูนย์วิทยทรัพยากร  
จุฬาลงกรณ์มหาวิทยาลัย



**Figure 4.9** Subtraction Laser Raman spectra of (A) 1% WO<sub>3</sub>/SBA-15, (B) 5% WO<sub>3</sub>/SBA-15, and (C) 10% WO<sub>3</sub>/SBA-15

## 4.2 Calcination Condition of Support and Supported Tungsten Catalysts

### 4.2.1 Effect of Time on Template Removal

XRD patterns and SEM images of as-synthesized SBA-15 and calcined SBA-15 are shown in Figure 4.10. Comparing the XRD pattern of as-synthesized SBA-15 with that of calcined SBA-15 at 500°C for 5 h, the intensity of the (100) peak was slightly increased from 7063 to 8778 cps respectively. This indicates that the template can not be removed from the pore of SBA-15 at 500°C for 5 h. While calcination at 500°C for 10 h, the template was completely removed from as-synthesized SBA-15 pores under such a condition. It results in two times increasing in intensity of the (100) peak from 7063 to 15366 cps of as-synthesized SBA-15 and calcined SBA-15, respectively. In addition, the calcined SBA-15 samples at 500°C for 5 and 10 h, (B) and (C), still have the rope-like morphology and remain rope-like morphology comparing with as-synthesized SBA-15. This indicates that removing template at high temperature and long time do not affect the morphology of SBA-15 support. Therefore, the calcination condition of 500°C for 10 h was selected in order to remove the template from as-synthesized SBA-15 pores.

ศูนย์วิจัยทรัพยากร  
จุฬาลงกรณ์มหาวิทยาลัย

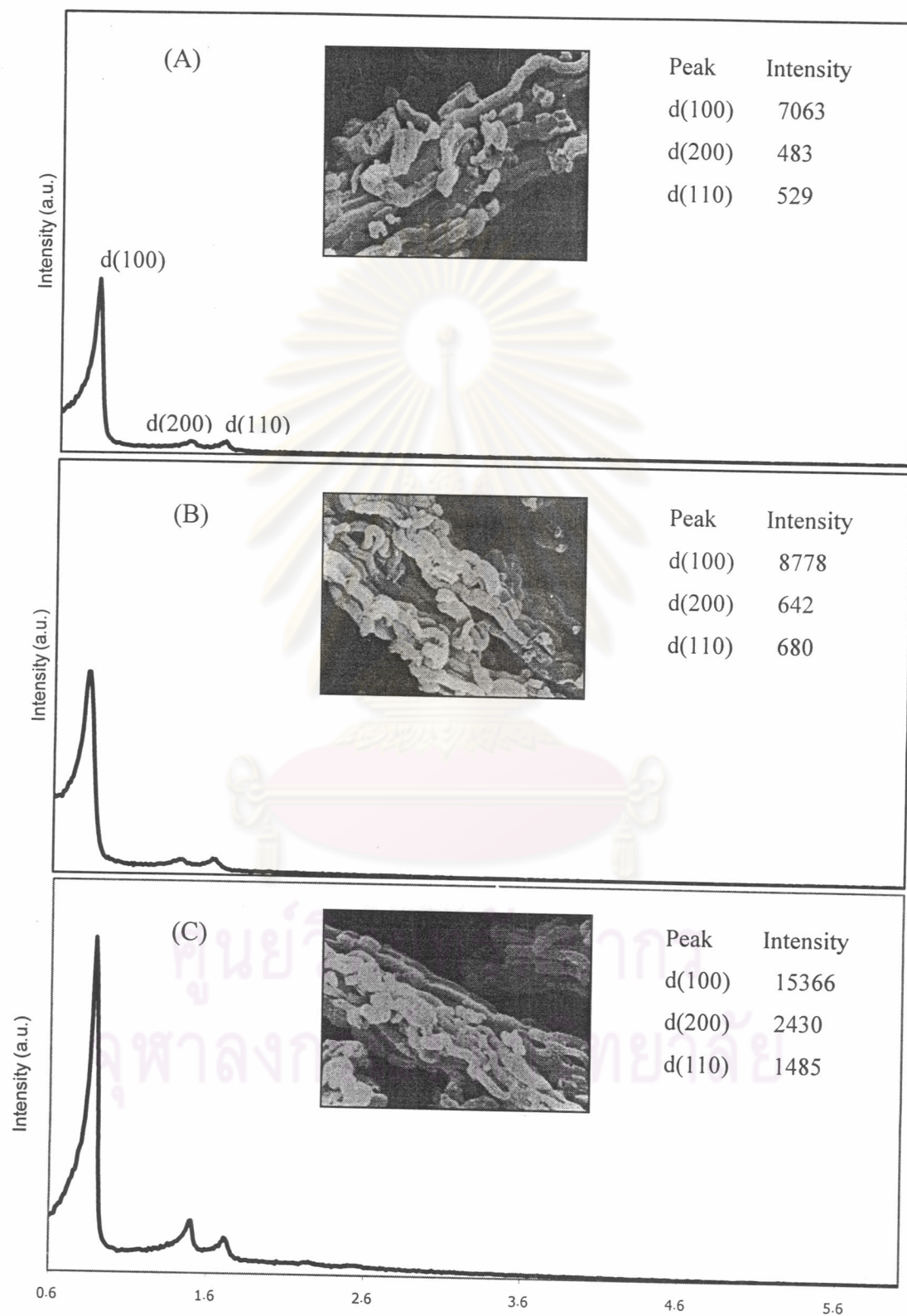


**Figure 4.10** XRD patterns and SEM images of (A) as-synthesized SBA-15 (B) calcined SBA-15 at 500°C for 5 h and (C) calcined SBA-15 at 500 °C for 10 h

#### 4.2.2 Effect of Moisture on Peak Intensity in XRD pattern of SBA-15

XRD pattern of as-synthesized SBA-15 samples before and after treatment at 100°C are shown in Figure 4.11 and the intensity values of the (100) reflection are summarized in Table 4.2. As described from Table 4.2, XRD peak intensities of sample B and C increase after as-synthesized SBA-15 (sample A) was dried at 100°C. However, there was no difference in the value after drying for 30 and 60. It indicates that the presence of moisture in as-synthesized SBA-15 results in lower XRD peak intensity of the (100) peak. Because the XRD peak intensity is very sensitive to moisture, when sample B and C were calcined at 500°C for 10 h, they show the increase in XRD peak intensity. It is in agreement with the results in section 4.2.1.

**Table 4.2** XRD peak intensity of as-synthesized SBA-15 before and after treatment at 100°C

Sample	Sample description	Peak intensity d(100)
A	As-synthesized SBA-15	4199
B	Sample A + dried at 100 °C for 30 min	8053
C	Sample A + dried at 100 °C for 60 min	7419
D	Sample B + calcine at 500 °C for 10 h	11760
E	Sample C + calcine at 500 °C for 10 h	11212

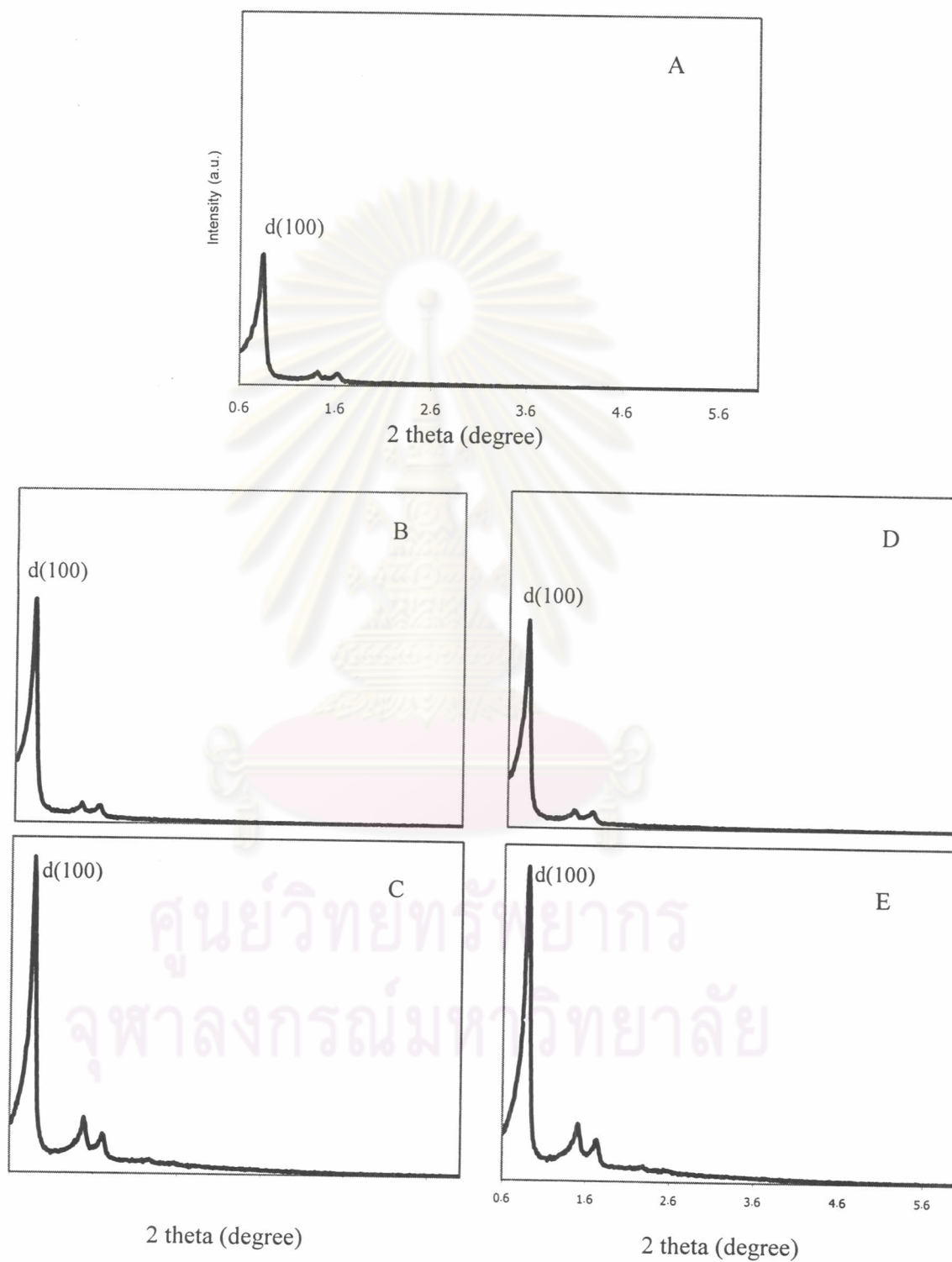


**Figure 4.11** XRD patterns of as-synthesized SBA-15 before and after treatment at 100°C ( Figure A-E refer to sample A-E in Table 4.2)



## 4.2 Catalytic Activities of WO<sub>3</sub>/SBA-15 Catalysts for Metathesis of 1-Hexene

### 4.2.1 Effect of Temperature on Catalytic Activities

The catalytic results for conversion of 1-hexene over WO<sub>3</sub>/SBA-15 at various reaction temperatures are shown in Table 4.3. With increasing reaction temperatures from 100 to 500 °C, conversion of 1-hexene increases from 15.50 to 93.30%, respectively. The selectivity to liquid phase increases from 30.68 to 61.21% with increasing temperature. In contrast, the selectivity to gas phase decreases from 68.68 to 22.87% with increasing temperature.

**Table 4.3** Catalytic activities of 5% WO<sub>3</sub>/SBA-15 catalyst in 1-hexene conversion at various temperatures, feed of 30.5% 1-hexene in nitrogen, time on stream of 30 min

	Reaction temperatures				
	100°C	200°C	300°C	400°C	500°C
Conversion of 1-hexene (%)	15.55	23.95	41.10	56.80	93.33
Selectivity to Gas products (%wt)	68.68	64.27	50.77	38.00	22.87
Selectivity to Liquid products (%wt)	30.68	34.54	44.95	55.35	64.21
Coke (%wt)	0.64	1.19	4.28	6.65	12.92

Gaseous product distribution obtained from using 5% WO<sub>3</sub>/SBA-15 as catalysts at various reaction temperatures is shown in Figure 4.13. Formation of methane and ethane is favored at high temperatures, 400 and 500 °C. This is due to cracking of hydrocarbons at elevated temperature. The temperature lower than 300 °C are not suitable for formation of ethylene and propylene while formation of butanes is preferable under such a condition. Although at the temperature from 400 to 500 °C high conversion of 1-hexene and high selectivity to ethylene are obtained, metathesis reaction was indeed competed by cracking process. Considering the product distribution at the temperature of 300°C, it shows reducing of cracking process which corresponds to low methane formation and still provides ethylene and propylene as major products. For these reasons, the temperature of 300 °C is a suitable condition for metathesis reaction of 1-hexene over WO<sub>3</sub>/SBA-15, with the objective to produce light olefins as well.

Considering liquid product distribution from Figure 4.14, the group of C<sub>5</sub> and C<sub>6</sub> are major products where alkenes are formed in higher amount than alkanes. However, it is not significantly different in amount of C<sub>5</sub> and C<sub>6</sub> in each group as temperature increases. C<sub>5</sub> and C<sub>6</sub> alkanes might be formed by thermal cracking process of heavier hydrocarbons which present in the system due to metathesis of 1-hexene. In addition, the liquid products in the group of C<sub>5</sub> alkenes were obtained from the metathesis reaction of 2-hexene and ethylene as shown in Figure 4.12.

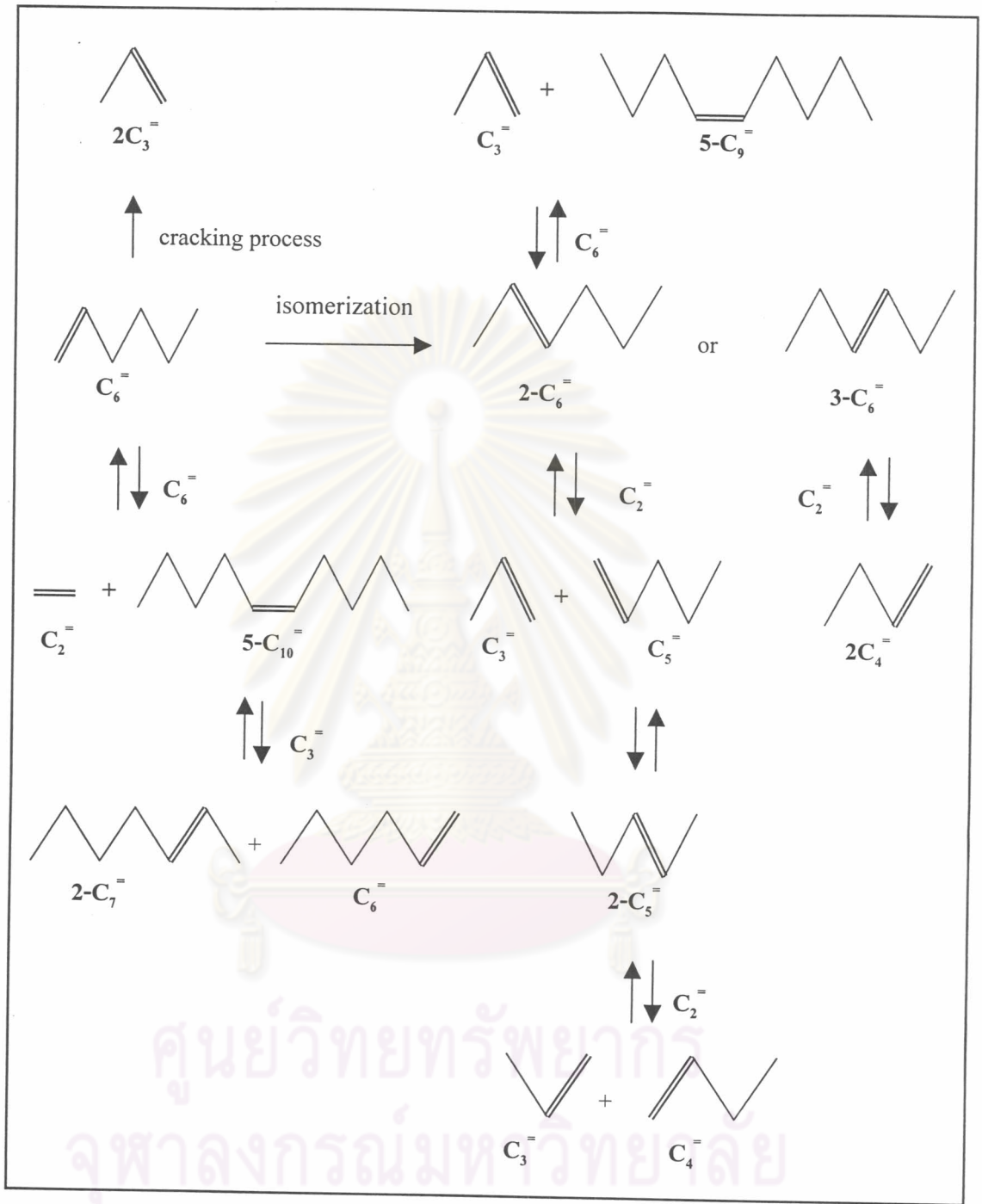
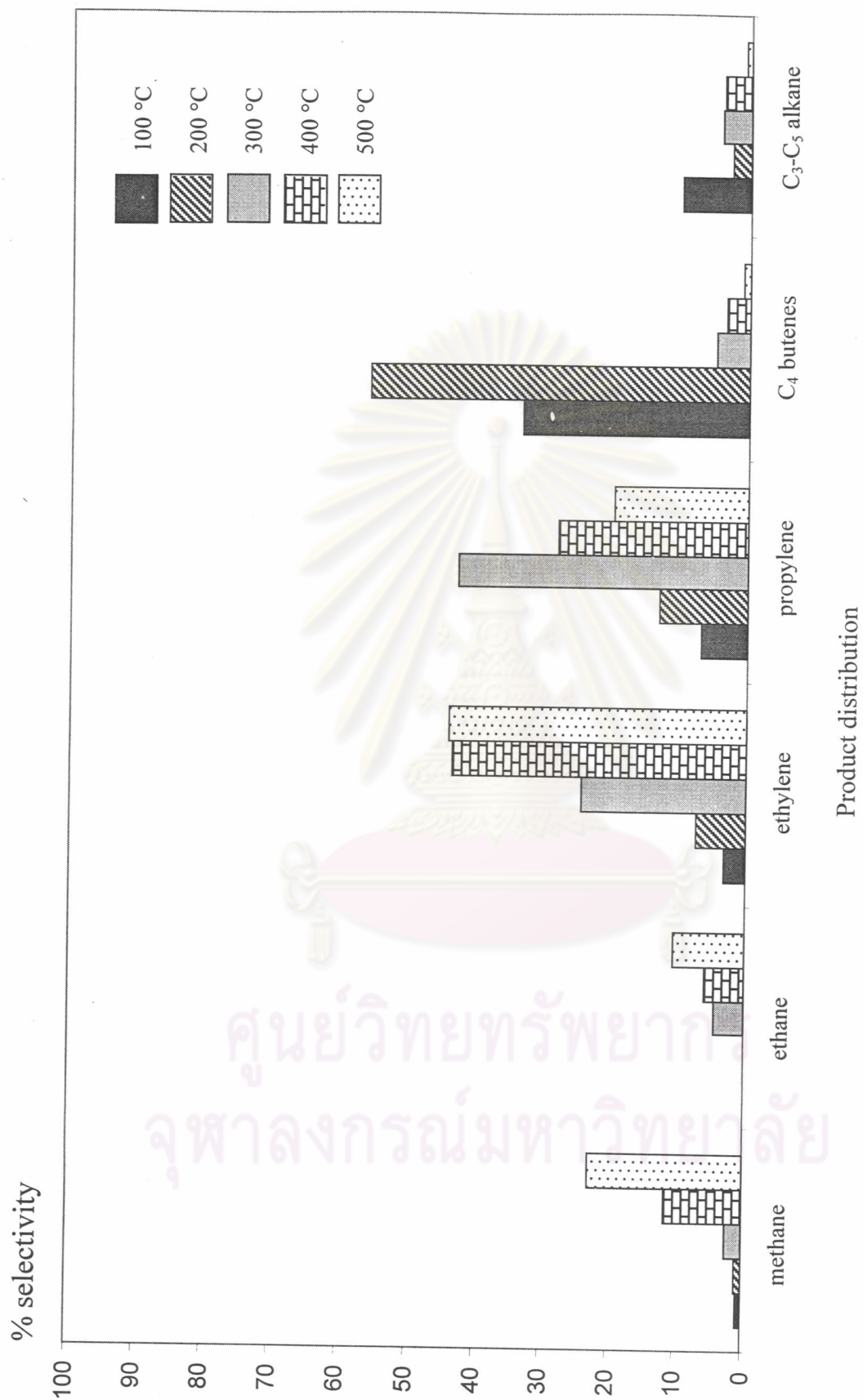
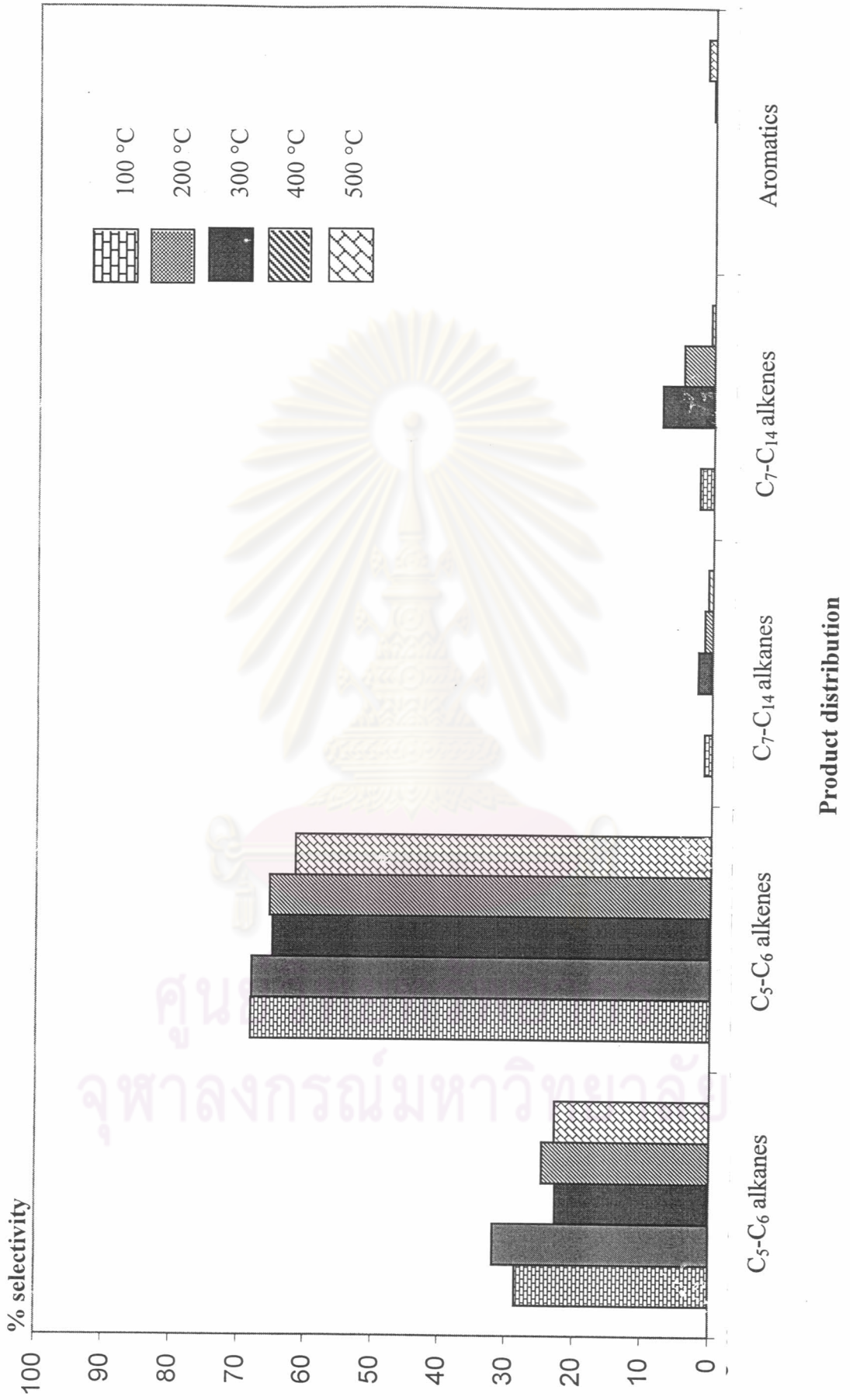


Figure 4.12 Reaction of 1-hexene during metathesis course



**Figure 4.13** Gas product distribution of 1-hexene conversion catalyzed by 5% WO<sub>3</sub>/SBA-15 at various reaction temperatures.

(GSHV = 500 h<sup>-1</sup>, time on stream = 30 min)



**Figure 4.14** Liquid product distribution of 1-hexene conversion catalyzed by 5% WO<sub>3</sub>/SBA-15 at various reaction temperatures. (GSHV = 500 h<sup>-1</sup>, time on stream = 30 min)

#### 4.2.2 Effect of WO<sub>3</sub> Loading on Catalytic Activities

The percentage conversions of 1-hexene over tungsten oxide supported catalyst at various loadings at temperature of 300 °C are listed in Figure 4.4. Increase in the tungsten loading results in higher conversion of 1-hexene from 14.65 to the maximum of 46.13% which decreasing with further increasing the loading amount higher than 5% WO<sub>3</sub>. The increase of WO<sub>3</sub> loading from 0 to 10% results in the increase of the selectivity to liquid phase from 33.68 to 86.38% but the selectivity to gas phase decreases from 55.87 to 10.45%. It is interested that coke formation decreases with increasing the percentage of WO<sub>3</sub>.

**Table 4.4** Catalytic activities WO<sub>3</sub>/SBA-15 catalyst in 1-hexene conversion at various percentage of WO<sub>3</sub>, feed of 30.5% 1-hexene in nitrogen, time on stream of 30 min at temperature of 300 °C

	% WO <sub>3</sub> loading					
	0	1	3	5	7	10
Conversion of 1-hexene (%)	14.65	19.40	25.55	41.10	44.05	34.15
Selectivity to gas products (%wt)	55.87	49.33	52.43	50.77	15.22	10.45
Selectivity to liquid products (%wt)	33.68	41.00	40.32	44.95	80.62	86.38
Coke (%wt)	10.45	9.67	7.25	4.28	4.16	3.17

Considering product distribution from Figure 4.15, the formation of methane decreases whereas the formation of ethane increases with increasing percentage of  $\text{WO}_3$ . This indicates that the increase in the  $\text{WO}_3$  amount results in less formation of methane from ethane and other hydrocarbons. At 1%  $\text{WO}_3$  loading, it seems to be no effect on the selectivity to the product. The product distribution of 1%  $\text{WO}_3$  loaded sample is similar to that of the bare support. As the percentage amount of  $\text{WO}_3$  increases from 3 to 10%, the difference in selectivity to light olefins can be observed. It is shown that the selectivity to ethylene increases with increasing the amount of  $\text{WO}_3$  loading on the support. The selectivity to propylene increases with increasing  $\text{WO}_3$  loading and reaches the maximum when the loading becomes 5%  $\text{WO}_3$ . Exceeding 5%  $\text{WO}_3$  loading results in the decrease of propylene selectivity. This might be due to pore clogging from the high amount of tungsten oxide, reducing in pore volume of the SBA-15 support. Simultaneously, high loading of  $\text{WO}_3$  on SBA-15 can be a driving force to form ethylene and butene via metathesis reaction of propylene. 1-Hexene can undergo metathesis reaction, in addition, it can be a primary source producing light olefins at elevated temperature. Light olefins,  $\text{C}_2$ - $\text{C}_4$  alkenes, can further undergo metathesis over the same catalyst.

It is difficult to avoid cracking of 1-hexene because the reaction temperature is much higher than its boiling point and perhaps decomposition point. However, at 300 °C, where the least cracking taking place, the self-metathesis of propylene to form ethylene and butene is preferable at the loading of 10%  $\text{WO}_3$  on SBA-15. The reverse process to convert ethylene and butene to propylene, that is called cross-metathesis, is favored at the loading of 5%  $\text{WO}_3$  on SBA-15.

Liquid product distribution are shown in Figure 4.16. The group of  $\text{C}_5$  and  $\text{C}_6$  products are also major products. As illustrated in Figure 4.16, increase in tungsten loading results in decreasing amount of  $\text{C}_5$  and  $\text{C}_6$  alkenes. This might be due to high

tungsten loading consists of large amount of catalytic sites, therefore  $C_5$  and  $C_6$  alkenes were readily reactive to these catalytic sites.  $C_5$  and  $C_6$  alkanes are formed due to cracking of heavier hydrocarbons which are formed via metathesis of 1-hexene.



ศูนย์วิทยทรัพยากร  
จุฬาลงกรณ์มหาวิทยาลัย



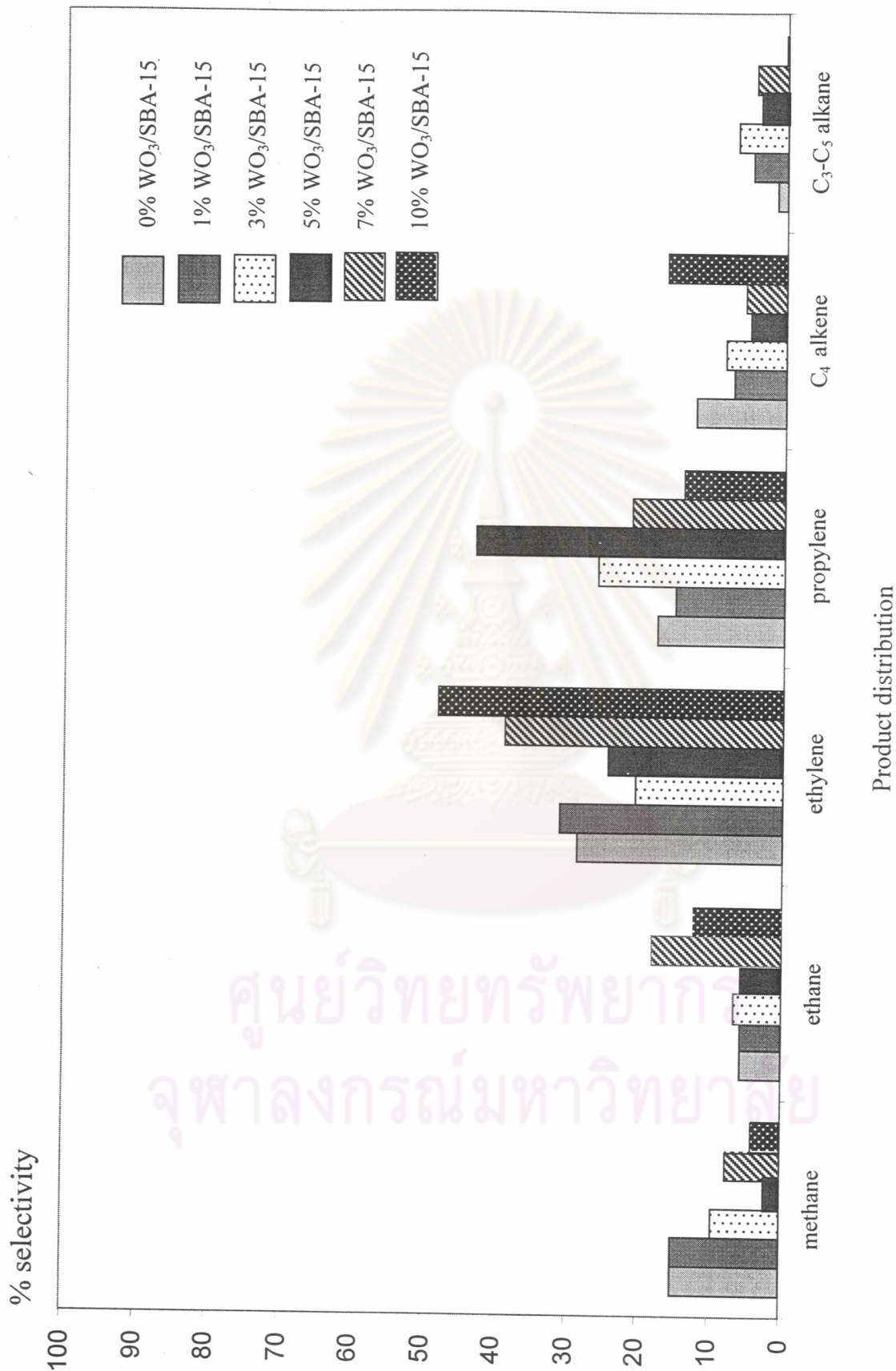


**Figure 4.15** Gas product distribution of 1-hexene conversion catalyzed by WO<sub>3</sub>/SBA-15 at various tungsten loadings. (T=300°C, GSHV = 500 h<sup>-1</sup>, time on stream = 30 min)

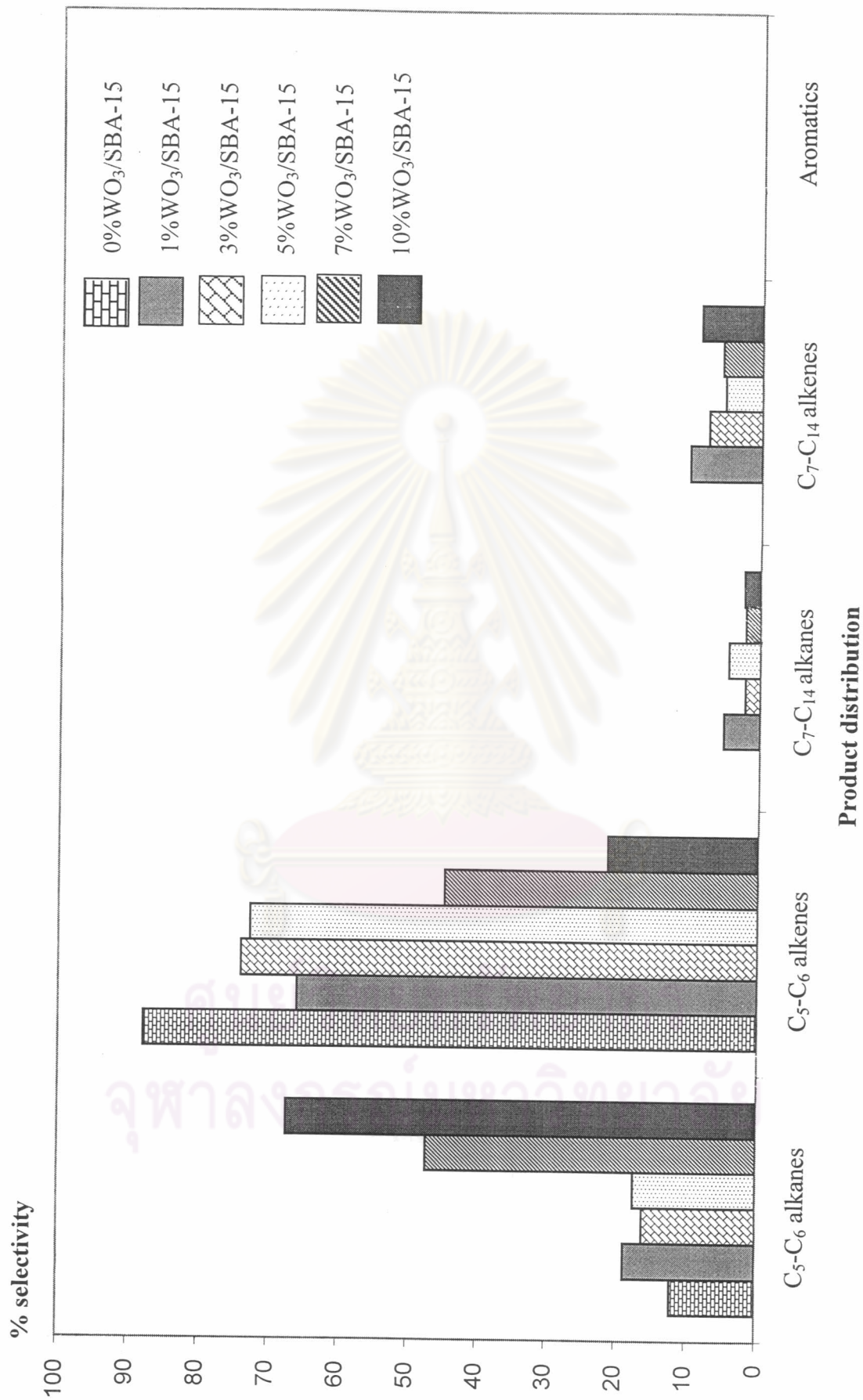


**Figure 4.16** Liquid product distribution of 1-hexene conversion catalyzed by WO<sub>3</sub>/SBA-15 at various tungsten loadings. (T = 300°C, GSHV = 500 h<sup>-1</sup>, time on stream = 30 min)